Geophysical Research Letters

RESEARCH LETTER
10.1029/2018GL080783

Special Section:
Atmospheric Rivers: Intersection of Weather and Climate

# Sensitivity of Seasonal Snowfall Attribution to Atmospheric Rivers and Their Reanalysis-Based Detection

**Laurie S. Huning[1], Bin Guan[2,3], Duane E. Waliser[3,2], and Dennis P. Lettenmaier[4]**

[1]Department of Civil and Environmental Engineering, University of California, Irvine, CA, USA, [2]Joint Institute for Regional Earth System Science and Engineering, University of California, Los Angeles, CA, USA, [3]Jet Propulsion Laboratory, California Institute of Technology, Pasadena, CA, USA, [4]Department of Geography, University of California, Los Angeles, CA, USA

**Key Points:**
- Atmospheric rivers (ARs) diagnosed with four atmospheric reanalyses often yield consistent mean seasonal snowfall patterns in the Sierra Nevada
- Higher-resolution atmospheric reanalyses diagnose up to four more ARs per winter implying 10% greater AR attribution to the mean seasonal snowfall
- Knowing how many snowy ARs occur per winter yields more information about the total seasonal snowfall than only knowing how many ARs occur

**Supporting Information:**
- Supporting Information S1

**Correspondence to:**
L. S. Huning,
lhuning@uci.edu

**Citation:**
Huning, L. S., Guan, B., Waliser, D. E., & Lettenmaier, D. P. (2019). Sensitivity of seasonal snowfall attribution to atmospheric rivers and their reanalysis-based detection. *Geophysical Research Letters*, *46*, 794–803. https://doi.org/10.1029/2018GL080783

Received 15 OCT 2018
Accepted 5 JAN 2019
Accepted article online 11 JAN 2019
Published online 24 JAN 2019



**Abstract** We characterize the sensitivity of atmospheric river (AR)-derived seasonal snowfall estimates to their atmospheric reanalysis-based detection over Sierra Nevada, USA. We use an independent snow data set and the ARs identified with a single detection method applied to multiple atmospheric reanalyses of varying horizontal resolutions, to evaluate orographic relationships and contributions of individual ARs to the seasonal cumulative snowfall (CS). Spatial resolution differences have relatively minor effects on the number of ARs diagnosed, with higher-resolution data sets identifying four more AR days per year, on average, during the 1985–2015 winters. However, this can lead to ~10% difference in AR attribution to the mean domain-wide seasonal CS and differences up to 47% snowfall attribution at the seasonal scale. We show that identifying snow-bearing ARs provides more information about the seasonal CS than simply knowing how many ARs occurred. Overall, we find that higher-resolution atmospheric reanalyses imply greater attribution of seasonal CS to ARs.

**Plain Language Summary** While it is known that elongated moisture-rich atmospheric features, known as atmospheric rivers (ARs), play an important role in the water resources of the mountainous western United States, less is known about how the atmospheric data sets used to diagnose the presence of ARs influence the amount of AR-attributed snowfall estimated each winter. Nonetheless, this missing information can be important for managing water resources and improving seasonal snowfall forecasts for areas depending on AR-derived snowfall. We show that using a single AR detection algorithm, applied to multiple atmospheric reanalyses to identify ARs, higher-resolution atmospheric reanalyses diagnose up to four more ARs per winter implying 10% greater AR attribution to the mean seasonal snowfall across Sierra Nevada, USA. Understanding how different atmospheric reanalyses play a role in our interpretation of AR impacts for hydrologic studies and water resources management, as we investigate here, is important especially as more ARs are projected to occur in a warmer future atmosphere.

## 1. Introduction

Atmospheric rivers (ARs) are elongated filaments of anomalous integrated horizontal water vapor transport that substantially influence the global water cycle and regional hydrology. They frequently cause intense precipitation and flooding across the western United States (Ralph et al., 2016) and also deliver beneficial rain and snow to the semiarid region that can help terminate drought conditions (Dettinger, 2013). As ARs interact with mountains, their precipitation, often occurring as snowfall, is orographically enhanced (Huning et al., 2017, hereafter H2017; Neiman et al., 2013). ARs contribute, on average, ~30–56% of the seasonal snowfall (defined as accumulated snow water equivalent, SWE, herein) that occurs over Sierra Nevada, USA (Guan et al., 2010, 2013; H2017), or roughly 35–66% of the average (1998–2015) peak SWE volume.

Several methods have been developed to identify ARs. Generally, they are based on using integrated water vapor and/or integrated vapor transport (IVT; Shields et al., 2018). They have been applied to satellite imagery, field observations, atmospheric reanalyses, and model output (e.g., Gershunov et al., 2017; Guan & Waliser, 2015, 2017; Neiman et al., 2009; Ralph et al., 2004; Rutz et al., 2014; Wick et al., 2013). The AR Tracking Method Intercomparison Project (Shields et al., 2018) challenges the community to better

understand how climatological, hydrological, and extreme impacts attributed to ARs are sensitive to different AR algorithms and other sources of uncertainty. Our present study, and its predecessor H2017, examines and quantifies these sensitivities in relation to AR-related cumulative snowfall (CS).

When considering AR-attributed snowfall, uncertainty results from (1) atmospheric data used to represent ARs, (2) AR detection methods, and (3) snow data. We focus on the first source of uncertainty to characterize how snowfall attribution is sensitive to the atmospheric reanalysis used to identify ARs. H2017 previously investigated the second source of uncertainty using a satellite-based integrated water vapor method (Neiman et al., 2008) and an atmospheric reanalysis-based IVT method (Guan & Waliser, 2015, hereafter GW2015) to show how snowfall attribution to ARs depends on the detection method used to diagnose ARs. They found that the average annual AR contribution to the total CS volume differed by >20% between the two methods since the number of winter ARs they diagnosed differed by a factor of ~2 over the Sierra Nevada. While snow information is another source of uncertainty, its role in AR-attributed snowfall estimates will be addressed in future work.

Here, we ask how sensitive hydrologic estimates are to the atmospheric data set used in AR detection and in particular, to alternative atmospheric reanalyses, which are the most common source of atmospheric data used by AR detection algorithms. Specifically, we consider the extent to which AR-derived snowfall over the Sierra Nevada is impacted by the choice of atmospheric reanalysis given a fixed AR detection algorithm, that of GW2015 (and a fixed set of detection parameters), and a specific snow data set. Previous studies have neither systematically examined the role that diagnoses from alternative atmospheric reanalyses play in AR snowfall estimates nor differentiated hydrologic implications, for example, how many ARs occurred versus those actually yielding snowfall.

## 2. Methods and Data

We use the following steps to attribute snowfall to ARs:

i Compute IVT from an atmospheric reanalysis between 1,000 and 300 hPa, inclusive (GW2015; Guan & Waliser, 2017).
ii Apply the GW2015 algorithm to diagnose ARs from IVT at 6-hourly time steps (section 2.1).
iii Identify the days ARs persist over the study domain (Figure S1 in the supporting information) to form the AR catalogs used here (section 2.1).
iv Use AR dates to extract the amount of snowfall that occurred on those days from an independent snow data set (sections 2.2–2.3).

We repeat these steps for each of the (four) atmospheric reanalyses. Steps ii–iv are further described below.

### 2.1. AR Diagnostics and Catalogs

We use the IVT-based AR detection algorithm GW2015, which (a) utilizes a seasonally and geographically varying 85th percentile IVT intensity threshold, (b) requires an overall coherence in the IVT direction across individual grid cells within an identified AR and consistency between the direction of mean IVT and the orientation of the AR shape, and (c) applies geometric constraints including a length-to-width ratio of >2 and a length of >2,000 km to diagnose AR conditions. We derive the AR catalogs using this algorithm applied to 6-hourly IVT fields from the following atmospheric reanalyses for water years 1985–2015: (1) National Centers for Environmental Prediction-National Center for Atmospheric Research reanalysis (NCEP-NCAR; Kalnay et al., 1996) at 2.5° × 2.5° resolution, (2) European Centre for Medium-Range Weather Forecasts Re-Analysis Interim (ERA-Interim; Dee et al., 2011) at 1.5° × 1.5°, (3) Modern-Era Retrospective Analysis for Research and Applications, version 2 (MERRA2; Bosilovich et al., 2015) at 0.5° × 0.625°, and (4) Climate Forecast System Reanalysis (CFSR; Saha et al., 2010) at 0.5° × 0.5°. We use the same set of algorithm parameters for all data sets. Only the input IVT data differs among the AR catalogs. Based on GW2015 and H2017, we define an AR day as a calendar day on which AR conditions persisted for ≥18 hr (i.e., three consecutive time steps) within or intersecting the outlined region in Figure S1. The "AR days" concept, used in previous studies (e.g., Dettinger et al., 2011; Guan et al., 2010; H2017; Kim et al., 2018; Neiman et al., 2008) and discussed in Text S1, facilitates the association with the daily resolved snowfall data (section 2.2) and accommodates the propagation of an AR over the study domain during the 24-hr period of snowfall accumulation.

Hereafter, we refer to these four catalogs as "main" catalogs to differentiate them from those we generated by coarsening the CFSR IVT to 1.5° and 2.5° grids to match ERA-Interim and NCEP-NCAR spatial resolutions, respectively, and repeating steps ii–iv above. We denote the resulting two catalogs as $CFSR_{1.5}$ and $CFSR_{2.5}$, respectively. They facilitate our investigation into how the horizontal resolution of IVT fields manifests in differences in the AR-derived CS. The number of ARs in all catalogs consistently decreases from northern to southern California (Figure S2). The differences in AR occurrence (number and timing) affect AR-related snowfall patterns, which we investigate below. To avoid introducing additional sources of uncertainty through temperature biases in the atmospheric reanalyses, their snowfall parameterizations, etc., we do *not* use CS estimates from any of these reanalyses. We *only* use these reanalyses to obtain AR dates. An external snow data set provides *all* of the snowfall information.

### 2.2. Snowfall Data

We determine snowfall using the 90-m, daily SWE fields from the Sierra Nevada snow reanalysis (Margulis et al., 2016), which was developed using a Bayesian framework and Landsat fractional snow-covered area imagery beginning in water year 1985. Based on Huning and Margulis (2017), CS accumulating over the winter season, defined as 1 November to 1 April, is computed by integrating daily increases in SWE (i.e., $\Delta SWE > 0$). Since the pixel-wise peak SWE volume is ~90% of the winter CS, on average, snowfall (in units of equivalent water) is nearly interchangeable with peak SWE in the mountainous Sierra Nevada interior, where most of California's snowpack accumulates in the winter. Huning and Margulis (2017) verified the derived CS with collocated snow pillows, finding mean and root-mean-square differences of −4 and 12 cm, respectively.

### 2.3. AR Snowfall Occurrence and Contribution

Using daily snowfall from the snow reanalysis and AR days information from the AR catalogs (sections 2.1 and 2.2), any snowfall that occurred on an AR day over the mountain range is attributed to the AR. We characterize the number of AR days, their seasonality, and CS contributions using the six AR catalogs. We compute the AR-derived CS (hereafter, AR CS) and the "non-AR CS" or the total (seasonal) CS minus the AR CS. To quantify the number of ARs yielding given amounts of CS, we define daily thresholds for AR CS of 1%, 5%, and 10% of the long-term average AR CS volume derived using each catalog. Since we examine these computations on a daily timescale, we only consider AR days. However, to address potential temporal differences in lag/lead times in the diagnosis of AR-derived CS when computing season totals, we integrate the snowfall accumulating on the diagnosed AR day(s) plus 1 day before and 1 day after the AR (without double counting). We use "CS-contributing days" (i.e., AR day ± 1 day) to compute the seasonal CS volume, fraction of the total CS attributed to ARs ($f_{AR}$), and orographic CS. H2017 showed the implications of using CS-contributing days versus only CS occurring on AR days. CS volume calculations include all basins shown in Figure S1. We characterize orographic CS (in equivalent water depth) only along the windward (western) basins in the northwest (NW) and southwest (SW) Sierra Nevada (Figure S1), which accumulate higher seasonal CS than the eastern side (Huning & Margulis, 2017).

## 3. Results and Discussion

### 3.1. Characterizing AR Days and Snowfall

The seasonality of ARs (Figure S3) is consistent across the catalogs with a consensus in heightened AR activity in the winter and specifically in January (~5–6 days/year). Given the larger number of winter ARs and the importance of snowfall accumulation, we exclusively examine the winter season (November to April) hereafter. Based on the four main catalogs, 22.6 (NCEP-NCAR) to 26.5 AR days/year (MERRA2) occur each winter, on average (Figure 1, top and bottom). MERRA2 exhibits the largest interannual variability in the number of ARs, having an interquartile range of 14.5 days/year, while the interannual variability of ERA-Interim diagnoses is only 60.3% of that of MERRA2. NCEP-NCAR diagnoses the fewest winter ARs annually (Figure 1, top), resulting in the least temporal agreement with diagnoses from these four catalogs (Text S2 and Figure S4). In general, the higher-resolution atmospheric reanalyses (MERRA2 and CFSR) identify more ARs than the coarser ones (ERA-Interim and NCEP-NCAR). We further explore this spatial resolution dependence of AR detection below.

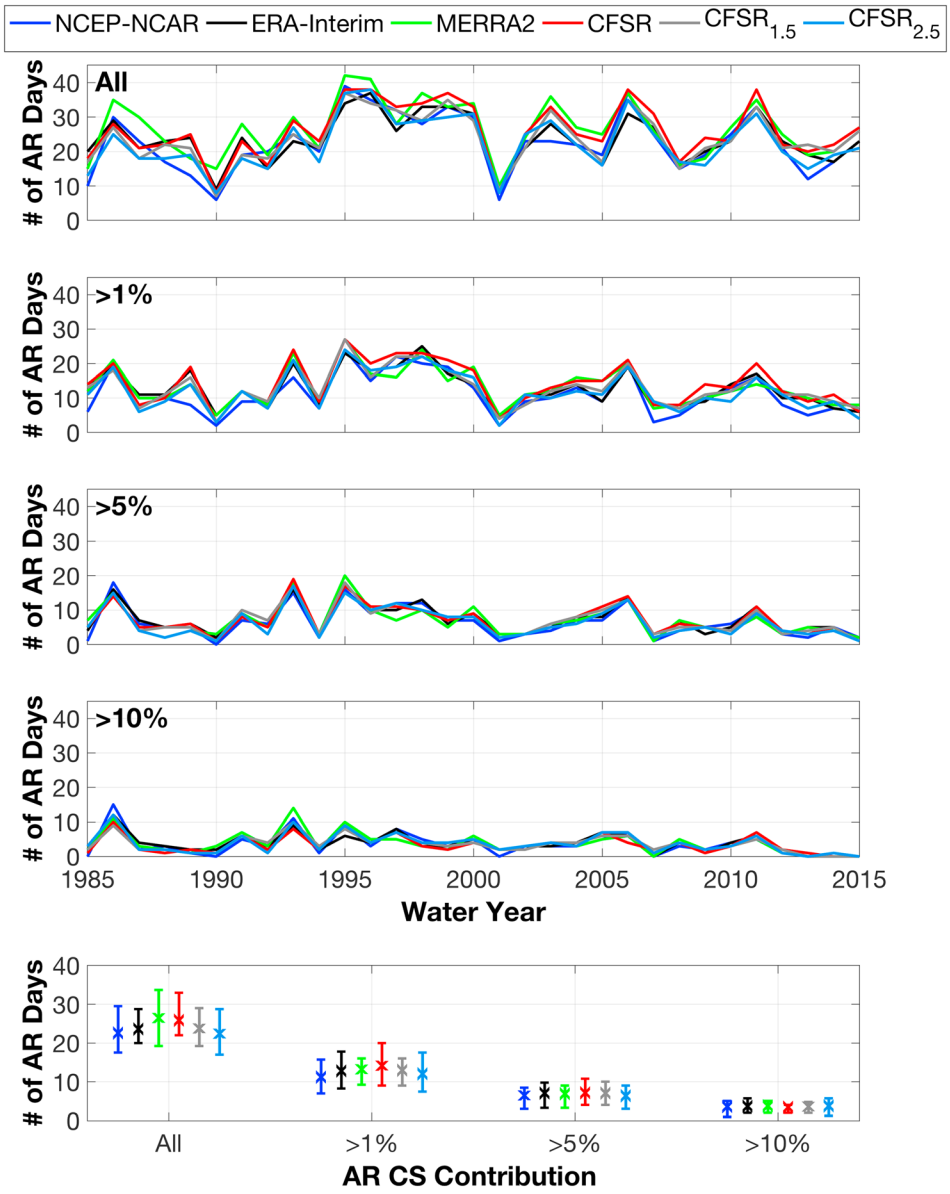


**Figure 1.** Number of AR days diagnosed during the winters of water years 1985–2015. (top) All AR days. (rows 2–4) AR days yielding >1%, >5%, and >10% of the long-term average seasonal AR CS occurring on AR days for each catalog, respectively. (bottom) Average number of AR days diagnosed ("x" symbols) and interquartile range (bars) for rows 1–4. AR = atmospheric river; CS = cumulative snowfall; NCEP-NCAR = National Centers for Environmental Prediction-National Center for Atmospheric Research reanalysis; ERA-Interim = European Centre for Medium-Range Weather Forecasts Re-Analysis Interim; MERRA2 = Modern-Era Retrospective Analysis for Research and Applications, version 2; CFSR = Climate Forecast System Reanalysis.

Of all six catalogs, strong, positive relationships exist among the number of winter AR days identified annually (i.e., $r \geq 0.87$, $p < 0.05$ in Table S1), showing consistent year-to-year variations across catalogs (Figure 1). However, the strongest correlations are not necessarily between catalogs derived at similar resolutions (Table S1). Thus, spatial resolution alone does not determine the year-to-year variations in the number of winter ARs diagnosed, although it is an important factor in determining the climatological mean.

#### 3.1.1. How Many ARs Yield Snowfall?

Figure 1 (rows 2–4) shows the number of AR days that yield >1%, >5%, and >10% of the long-term average CS that occurs only on AR days, respectively. These criteria correspond to ~0.4%, 1.9%, and 3.8% of the long-term average total seasonal CS volume (22.4 $km^3$), respectively. As the minimum daily CS contribution from

ARs increases from rows 2 to 4 in Figure 1, the number of days meeting the minimum daily AR CS thresholds converges across the catalogs and the associated interannual variability and spread among catalogs decreases. Figure 1 (bottom) illustrates that the influence of the horizontal resolution on the climatological mean diminishes as the intensity (in terms of CS) of the ARs increase; however, considering the interquartile ranges, the differences among the catalogs are within the uncertainty of the data.

Figure 1 (bottom) demonstrates that, on average, 11–14 AR days per winter (~49–55% of the long-term average number of all AR days per winter) each yield >1% of the average total seasonal CS occurring on AR days, while 6–7 days (~28–30%) each yield >5% and 3–4 days (~13–17%) each yield >10%. The ranges indicate the variations/spread among the data sets here and after. Since on average ~3–4 days/year each yield >10% of the snowfall accumulating on AR days alone, this amounts to an average CS volume of 4.7–5.2 $km^3$/year, which is 52–64% of the long-term seasonal average AR CS occurring on AR days or ~21–23% of the long-term average total CS. Therefore, a large amount of AR-derived snowfall occurs over relatively few days (Guan et al., 2010). These findings complement those of Huning and Margulis (2017) who showed that, on average, the Sierra Nevada's basins (Figure S1) receive >50% of their total CS over ~6 of their highest accumulation days/year during snowstorms, not specifically ARs. The interannual variability and spread in the number of ARs that yield at least these minimum daily rates typically decrease as the threshold increases (Figure 1, row 5). We also observe greater consistency in the monthly distribution of ARs as the threshold increases (Figure S5). Stronger temporal agreement for larger ARs (Figure S4 and S5) leads to better agreement among the mean and interquartile ranges across catalogs (Figure 1).

Correlating the number of ARs in each row of Figure 1 (by catalog) with the corresponding derived AR CS for each year (characterized in section 3.3 and includes CS-contributing days) reveals that knowing the number of AR days yielding specified amounts of CS is a better predictor of the AR CS than simply knowing how many AR days occur (Table S2) since not all ARs (equally) deliver CS. Correlation values are stronger by ~0.01, on average, when only CS occurring on AR days is considered (not shown). Although the largest associations are typically for the 5% threshold, we observe strong relationships for the 1% and 10% thresholds. The 10% threshold results in more years with no ARs meeting the criterion, which can degrade the correlations relative to the 5% case. Similar associations are found between the number of AR days meeting the criteria and the total seasonal CS (Table S3). While there is some information content in the total number of AR days, knowing the number of AR days exceeding a given intensity (e.g., in terms of water vapor transport or other precipitation-related characteristics) provides more information about the total CS and AR-derived CS across the region.

Given similar distributions of the number of ARs (mean, variability, and seasonality) among the various catalogs, AR temperature differences are not expected to play a systematic role in snowfall attribution. Nonetheless, the differences that do exist among the catalogs can influence AR CS accumulation and attribution, which is our focus below.

### 3.2. Characterizing Seasonal Orographic Snowfall Distributions

Orographic enhancement of CS is promoted by abundant moisture and strong winds oriented perpendicular to a mountain slope (Huning & Margulis, 2018; Roe, 2005; Smith, 1979), or specifically, strong IVT, which characterizes ARs approaching the Sierra Nevada. Figure 2 (left; solid lines) shows that the derived elevational distributions of the long-term average AR CS have the largest values for ARs in the CFSR and MERRA2 catalogs. Since these two data sets have the most ARs and similar AR CS distributions, their attributed AR contributions to the total CS are comparable (Figure 2, right), particularly in the NW. In contrast, NCEP-NCAR diagnosed the fewest ARs, leading to the lowest derived AR CS at each elevation (Figure 2) and resulting in a larger proportion of the total CS attributed to non-AR snowfall mechanisms (dashed lines in Figure 2, left). At elevations above 2,000 m, the shapes of the AR and non-AR CS curves diverge with the non-AR CS curves taking on nearly constant values (Figure 2, left) and the AR CS comprising a large fraction of the total seasonal CS (i.e., $f_{AR}$ is 53–67% [NW] and 45–65% [SW]; Figure 2, right). Consequently, in this elevational range, the shapes of the AR CS curves more closely resemble the total CS curves (Huning & Margulis, 2018) since ARs yield a substantial amount of CS each season (section 3.1.1).

From lowest to highest elevations in the NW, the long-term average AR CS depth ranges from 12.2–15.6 cm to 65.6–73.6 cm, respectively (Figure 2, top left). The spread in AR CS depths increases with height from ~3.5

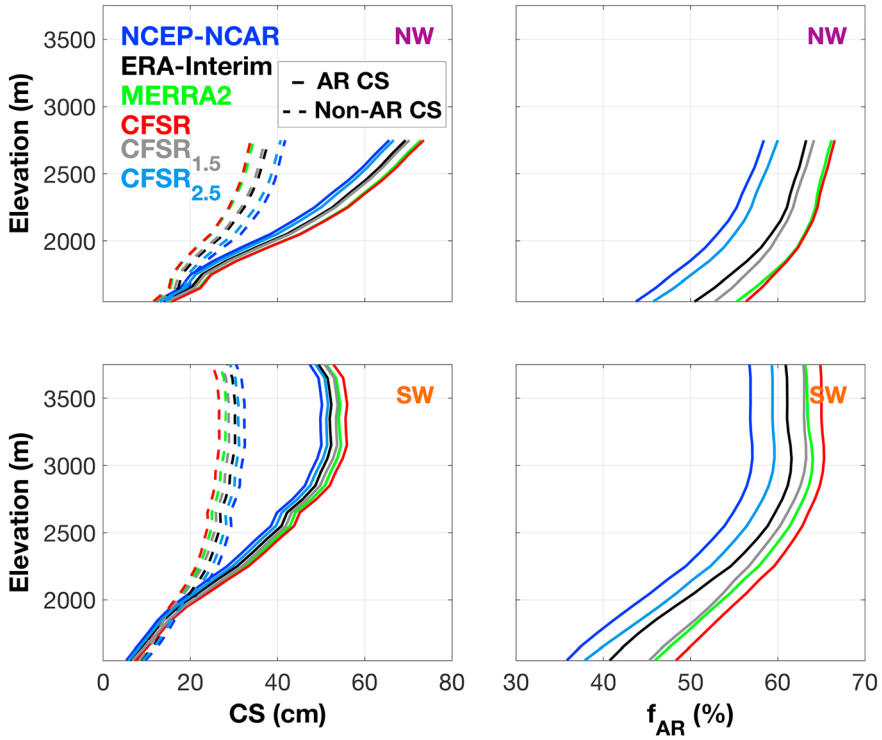


**Figure 2.** Distributions of the long-term average seasonal (left column) AR and non-AR CS depth and (right column) fraction of total CS attributed to ARs ($f_{AR}$) for the NW (top row) and SW (bottom row) Sierra Nevada. Here, AR CS is derived using CS-contributing days. Solid (dashed) lines demarcate AR (non-AR) CS in the left column. Elevation bins shown represent >0.5% of the (regional) area above 1,500 m (see Huning & Margulis, 2017). AR = atmospheric river; CS = cumulative snowfall; NCEP-NCAR = National Centers for Environmental Prediction-National Center for Atmospheric Research reanalysis; ERA-Interim = European Centre for Medium-Range Weather Forecasts Re-Analysis Interim; MERRA2 = Modern-Era Retrospective Analysis for Research and Applications, version 2; CFSR = Climate Forecast System Reanalysis.

to 7.9 cm, which is related to the general increase in the interannual variability of the AR CS with elevation (Figure S6, top left). Non-AR CS values exhibit similar relationships with their magnitudes and spread (Figure 2, top left) and interannual variability (Figure S6, top right) increasing with elevation. The AR CS depth in the relatively higher-elevation SW (Figure 2, bottom left) ranges from 5.3–7.2 cm (lowest elevation) to 50.2–56.0 cm (peak AR CS) with slightly lower variability (~2–6 cm spread) than in the NW using CS-contributing days from the main catalogs. The spread increases with elevation but reverses at the highest elevations. Similar shapes are observed in the corresponding interannual variability profiles of AR and non-AR CS (Figure S6, bottom row), although the interannual variability of the AR CS (left) is greater than for the non-AR CS (right). Factors, such as atmospheric moisture depletion that occurs at the highest elevations in the SW, control the increasing and then decreasing shape of these AR CS profiles (Huning & Margulis, 2018).

The long-term average $f_{AR}$ (Figure 2, right) ranges from 44–56% in the NW and 36–48% in the SW at the lowest elevations to 58–67% and 57–65% at the highest elevations in the respective regions. The difference in $f_{AR}$ values across data sets decreases with elevation from 12.6% to 8.1% in both regions as opposed to being >20% over all elevations as H2017 found using two different detection methods. In comparison to that study, the spread in the CS attribution, although still sizeable, is substantially reduced here. Thus, the differences arising from the choice of the AR detection method can be larger than those arising from the selection of the atmospheric data used for identifying ARs. Quantifying the range in $f_{AR}$ estimates provides a critical step toward improving AR diagnostics and understanding their implications, especially given the stronger associations between the number of snow-bearing ARs and the total seasonal CS (Table S3). Additionally, Text S3 and Figure S7 indicate that the climatological rate of change of AR CS with elevation is consistently greater than for non-AR CS mechanisms. Hence, changes in the number of snow-bearing ARs and the

amount of snowfall they deliver may greatly impact the total snowfall distribution and subsequently water resources.

#### 3.2.1. Influence of Horizontal Resolution on Orographic Snowfall Distributions

The long-term average profiles associated with the four main catalogs in Figures 2 and S7 are inherently ordered based on the spatial resolution of the diagnoses. The AR CS and $f_{AR}$ profiles indicate that larger amounts of CS are attributed to ARs when ARs are derived from higher-resolution atmospheric reanalyses (Figure 2). Although snowfall is taken from an external data set, the geometric length-to-width requirements can result in the horizontal resolution of the IVT fields playing a role in AR detection. If the length-to-width ratio becomes <2, an IVT object will not be identified as an AR and the horizontal resolution can thereby translate into differences in the number of diagnosed ARs among atmospheric reanalyses if others have identified AR conditions (GW2015). This can cause discernable differences at the impact level (i.e., snowfall attribution).

Considering $CFSR_{1.5}$ and $CFSR_{2.5}$ alongside the four main catalogs in Figures 2 and S7, we further investigate resolution as a driver of the spread among estimates. $CFSR_{1.5}$ and $CFSR_{2.5}$ profiles consistently lie closest to the curves associated with AR diagnoses at their same resolution or between that curve and the next finer one. Hence, at 1.5° (2.5°) resolution, the $CFSR_{1.5}$ ($CFSR_{2.5}$) profiles have values closest to those of ERA-Interim (NCEP-NCAR) or between ERA-Interim and MERRA2 (NCEP-NCAR and ERA-Interim). Furthermore, a 0.125° longitudinal difference between the MERRA2 and CFSR resolutions leads to similar derived values. As Figure 2 (right) highlights, coarser atmospheric reanalyses lead to greater winter snowfall attribution to non-AR mechanisms than finer ones (e.g., $f_{AR}$ at all elevations). Distinct resolution-dependent relationships are observable across all elevations given differences in the number and timing of diagnosed ARs (Figure S2–S5).

With the alignment of profiles based on the spatial resolution of the AR diagnoses, it follows that differences among the atmospheric reanalyses exert less influence on the profiles in Figure 2 than resolution since the profiles are similar between those derived using ARs diagnosed at comparable scales. The detection resolution does not solely dictate attribution patterns because variability exists among profiles of comparable scales, but it is low compared to differences between profiles based on largely different atmospheric resolutions (e.g., 0.5° vs. 2.5°). The profiles in Figure 2 generated using the ARs diagnosed from CFSR-derived catalogs yield larger AR CS values than from other sources at the same resolution. Although the maps in Figure S2 look similar between both 1.5° catalogs and both 2.5° catalogs, Figure S4 (top) indicates that temporally, the coarsened CFSR catalogs best agree with MERRA2 and CFSR-based catalogs. Therefore, the derived snowfall patterns using the coarsened catalogs yield higher AR CS values than using other catalogs derived at the same resolution. This may reflect underlying characteristics influenced by model parameterizations, assimilated data sources, etc.

### 3.3. Temporal Variability of AR CS

The seasonal AR CS (top) and $f_{AR}$ (bottom) time series in Figure 3a depict the spread across AR CS values and interannual variability derived using each catalog, which are quantified in Figure 3b. For a given year, the range in the AR CS and/or $f_{AR}$ values can be large (Figure 3a). Ten years have AR CS differences >5 $km^3$ with 1 year having differences up to 11 $km^3$ (2005). Furthermore, 8 years have $f_{AR}$ differences >20%, with 1990 and 2007 reaching ~41% and 47%, respectively. A correlation of 0.49 ($p < 0.05$) between the range of AR CS values and the total CS each year indicates that greater uncertainty among the AR CS values tends to occur during snowier years. Across all years and data sets, the average AR CS volume is 13.4 $km^3$ with an interannual variability (i.e., interquartile range) of ~10 $km^3$.

The interannual variability of the AR CS (Figure 3b, top left) is large given interquartile ranges that are 69–79% of their respective mean AR CS values, consistent with the generally large coefficient of variation in annual precipitation in this region (Dettinger et al., 2011, their Figure 3a). The AR CS volume has a mean value ranging from 12.3 to 14.3 $km^3$ with an interquartile range of 9.4 to 10.9 $km^3$ for NCEP-NCAR and CFSR, respectively. Since the average $f_{AR}$ values are >50% (Figure 3b, top right), the AR CS and total CS are strongly correlated. Approximately 72% (NCEP-NCAR) to 87% (CFSR) of the interannual variance in the total CS is explained by the variability in AR CS. This is consistent with Dettinger (2016) who found that year-to-year variations in total precipitation across California are largely attributable to a

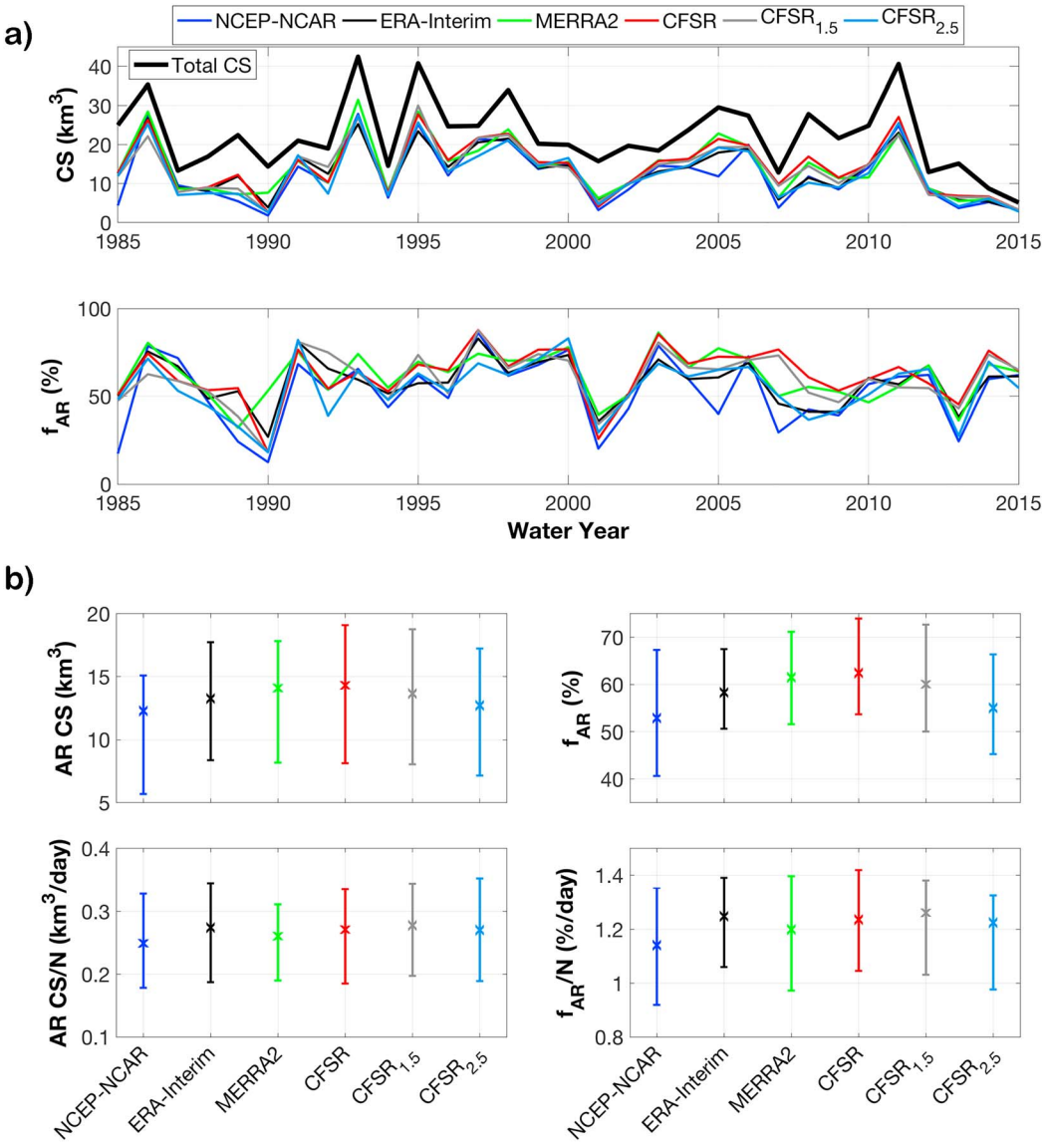


**Figure 3.** Seasonal CS volume and $f_{AR}$ time series and statistics. (a) AR CS (thin lines) using the CS-contributing days from each AR catalog and total CS (thick line) and $f_{AR}$, respectively. (b) Top row: Mean ("x" symbols) and interquartile range (bars) for AR CS and $f_{AR}$, respectively. Bottom row: Same as the top row in (b) except normalized by the number of winter CS-contributing days ($N$) for each catalog. AR = atmospheric river; CS = cumulative snowfall; NCEP-NCAR = National Centers for Environmental Prediction-National Center for Atmospheric Research reanalysis; ERA-Interim = European Centre for Medium-Range Weather Forecasts Re-Analysis Interim; MERRA2 = Modern-Era Retrospective Analysis for Research and Applications, version 2; CFSR = Climate Forecast System Reanalysis.

small number of most extreme precipitation days. On average, ARs contribute 52.9–62.4% of the total seasonal CS, a difference of ~10% across all data sets (Figure 3b, top right). Figure 3b (top) reinforces the tendency of the higher-resolution data sets to attribute greater seasonal importance to ARs than the coarser ones.

Since Figures 2, S7, 3a, and 3b (top) show distinct sensitivity among the derived CS relationships to the resolution of the IVT fields, we normalized the AR CS and $f_{AR}$ values by the number of CS-contributing days each winter (Figure 3b, bottom). Normalizing reduces the spread of the AR CS and $f_{AR}$ per day values. The range in the long-term average AR CS ($f_{AR}$) values is 15.3% (16.4%) of the mean of the long-term average values across data sets, whereas the range in normalized long-term AR CS ($f_{AR}$) values is 10.8% (9.9%) of its corresponding mean long-term average value.

## 4. Conclusions

We characterize the sensitivity of AR-attributed snowfall patterns to the atmospheric reanalyses used for identifying AR conditions, to illustrate how different atmospheric data can influence the interpretation of AR impacts for hydrologic studies. AR algorithms have previously been applied to a variety of atmospheric reanalyses (Guan & Waliser, 2017), but information about the hydrological implications of such applications over snow-covered mountains has been missing. Utilizing a single detection method, namely, the GW2015 IVT-based algorithm, we find reasonable agreement among the AR-attributed CS values using external snow data and ARs identified by four atmospheric reanalyses. While the derived snowfall patterns are consistent across data sets, large differences can arise at the seasonal-scale (e.g., domain-wide AR CS volume differences up to 11 $km^3$ and 47% attribution, Figure 3) and climatological-scale (e.g., elevational differences of $f_{AR}$ from 8% to 13%, Figure 2). Among the four atmospheric reanalyses we examine, snowfall attribution to ARs is sensitive to their horizontal resolution. However, the differences among the reanalyses are reduced when the higher-resolution reanalysis is coarsened to a common horizontal resolution prior to applying the AR detection algorithm (Figures 2 and 3).

Higher-resolution atmospheric reanalyses identify more AR days (Figure 1), leading to greater attributed importance of ARs to the seasonal CS and thereby larger AR CS accumulation than coarser ones (Figures 2 and 3). Snowier ARs are consistently identified regardless of the resolution; however, higher-resolution atmospheric reanalyses/catalogs identify smaller ARs that can yield CS (Figure 1, bottom). We show that identifying the snowiest AR days (Figure 1) provides more information about the total seasonal CS than diagnosing all ARs (Table S3). Our findings have potential applications in work aiming to better characterize the role of ARs in hydrology and intercomparison efforts such as the AR Tracking Method Intercomparison Project. Additional studies, involving historical analyses, climate studies, and near-term weather and seasonal forecasts are necessary to understand potential implications associated with AR attribution in other hydrological variables using multiple atmospheric data sets and AR methods. Such efforts should provide more comprehensive uncertainty quantification and thus better informed decision-making, water resources assessments, and modeling applications from local to global scales.

**Acknowledgments**
This work was partially supported by the NSF Earth Sciences Postdoctoral Fellowship EAR-1725789. The contribution of D. E. W. was carried out on behalf of the Jet Propulsion Laboratory, California Institute of Technology, under a contract with NASA. The AR catalogs and snow reanalysis are available at https://ucla.box.com/ARcatalog and https://margulis-group.github.io/data, respectively.

## References

Bosilovich, M. G., Akella, S., Coy, L., Cullather, R., Draper, C., Gelaro, R., et al. (2015). MERRA-2: Initial evaluation of the climate, technical report series on global modeling and data assimilation (NASA/TM-2015-104606/, Vol. 43, 139 pp.). Greenbelt, MD. Retrieved from https://gmao.gsfc.nasa.gov/pubs/docs/Bosilovich803.pdf

Dee, D. P., Uppala, S. M., Simmons, A. J., Berrisford, P., Poli, P., Kobayashi, S., et al. (2011). The ERA-Interim reanalysis: Configuration and performance of the data assimilation system. *Quarterly Journal of the Royal Meteorological Society*, *137*(656), 553–597. https://doi.org/10.1002/qj.828

Dettinger, M. D. (2013). Atmospheric rivers as drought busters on the U.S. West Coast. *Journal of Hydrometeorology*, *14*(6), 1721–1732. https://doi.org/10.1175/JHM-D-13-02.1

Dettinger, M. D. (2016). Historical and future relations between large storms and droughts in California. *San Francisco Estuary & Watershed Science*, *14*(2). https://doi.org/10.15447/sfews.2016v14iss2art1

Dettinger, M. D., Ralph, F. M., Das, T., Neiman, P. J., & Cayan, D. R. (2011). Atmospheric rivers, floods, and the water resources of California. *Water*, *3*(2), 445–478. https://doi.org/10.3390/w3020445

Gershunov, A., Shulgina, T., Ralph, F. M., Lavers, D. A., & Rutz, J. J. (2017). Assessing the climate-scale variability of atmospheric rivers affecting western North America. *Geophysical Research Letters*, *44*, 7900–7908. https://doi.org/10.1002/2017gl074175

Guan, B., Molotch, N. P., Waliser, D. E., Fetzer, E. J., & Neiman, P. J. (2010). Extreme snowfall events linked to atmospheric rivers and surface air temperature via satellite measurements. *Geophysical Research Letters*, L20401. https://doi.org/10.1029/2010GL044696

Guan, B., Molotch, N. P., Waliser, D. E., Fetzer, E. J., & Neiman, P. J. (2013). The 2010/2011 snow season in California's Sierra Nevada: Role of atmospheric rivers and modes of large-scale variability. *Water Resources Research*, *49*, 6731–6743. https://doi.org/10.1002/wrcr.20537

Guan, B., & Waliser, D. E. (2015). Detection of atmospheric rivers: Evaluation and application of an algorithm for global studies. *Journal of Geophysical Research: Atmospheres*, *120*, 12,514–12,535. https://doi.org/10.1002/2015JD024257

Guan, B., & Waliser, D. E. (2017). Atmospheric rivers in 20 year weather and climate simulations: A multimodel, global evaluation. *Journal of Geophysical Research: Atmospheres*, *122*, 5556–5581. https://doi.org/10.1002/2016JD026174

Huning, L. S., & Margulis, S. A. (2017). Climatology of seasonal snowfall accumulation across the Sierra Nevada (USA): Accumulation rates, distributions, and variability. *Water Resources Research*, *53*, 6033–6049. https://doi.org/10.1002/2017WR020915

Huning, L. S., & Margulis, S. A. (2018). Investigating the variability of high-elevation seasonal orographic snowfall enhancement and its drivers across Sierra Nevada, California. *Journal of Hydrometeorology*, *19*(1), 47–67. https://doi.org/10.1175/JHM-D-16-0254.1

Huning, L. S., Margulis, S. A., Guan, B., Waliser, D. E., & Neiman, P. J. (2017). Implications of detection methods on characterizing atmospheric river contribution to seasonal snowfall across Sierra Nevada, USA. *Geophysical Research Letters*, *44*, 10,445–10,453. https://doi.org/10.1002/2017GL075201

Kalnay, E., Kanamitsu, M., Kistler, R., Collins, W., Deaven, D., Gandin, L., et al. (1996). The NCEP/NCAR 40-year reanalysis project. *Bulletin of the American Meteorological Society*, *77*(3), 437–471. https://doi.org/10.1175/1520-0477(1996)077<0437:TNYRP>2.0.CO;2

Kim, J., Guan, B., Waliser, D. E., Ferraro, R. D., Case, J. L., Iguchi, T., et al. (2018). Winter precipitation characteristics in western US related to atmospheric river landfalls: Observations and model evaluations. *Climate Dynamics*, *50*(1-2), 231–248. https://doi.org/10.1007/s00382-017-3601-5

Margulis, S., Cortés, G., Girotto, M., & Durand, M. (2016). A Landsat-era Sierra Nevada (USA) snow reanalysis (1985–2015). *Journal of Hydrometeorology*, *17*(4), 1203–1221. https://doi.org/10.1175/JHM-D-15-0177.1

Neiman, P. J., Hughes, M., Moore, B. M., Ralph, F. M., & Sukovich, E. M. (2013). Sierra barrier jets, atmospheric rivers, and precipitation characteristics in northern California: A composite perspective based on a network of wind profilers. *Monthly Weather Review*, *141*(12), 4211–4233. https://doi.org/10.1175/MWR-D-00112.1

Neiman, P. J., Ralph, F. M., Wick, G. A., Lundquist, J. D., & Dettinger, M. D. (2008). Meteorological characteristics and overland precipitation impacts of atmospheric rivers affecting the West Coast of North America based on eight years of SSM/I satellite observations. *Journal of Hydrometeorology*, *9*(1), 22–47. https://doi.org/10.1175/2007JHM855.1

Neiman, P. J., White, A. B., Ralph, F. M., Gottas, D. J., & Gutman, S. I. (2009). A water vapour flux tool for precipitation forecasting. *Water Management*, *162*(2), 83–94. https://doi.org/10.1680/wama.2009.162.2.83

Ralph, F. M., Cordeira, J. M., Neiman, P. J., & Hughes, M. (2016). Landfalling atmospheric rivers, the sierra barrier jet, and extreme daily precipitation in northern California's Upper Sacramento River watershed. *Journal of Hydrometeorology*, *17*(7), 1905–1914. https://doi.org/10.1175/JHM-D-15-0167.1

Ralph, F. M., Neiman, P. J., & Wick, G. A. (2004). Satellite and CALJET aircraft observations of atmospheric rivers over the eastern North Pacific Ocean during the winter of 1997/98. *Monthly Weather Review*, *132*(7), 1721–1745. https://doi.org/10.1175/1520-0493(2004)132<1721:sacaoo>2.0.co;2

Roe, G. H. (2005). Orographic precipitation. *Annual Review of Earth and Planetary Sciences*, *33*(1), 645–671. https://doi.org/10.1146/annurev.earth.33.092203.122541

Rutz, J. J., Steenburgh, W. J., & Ralph, F. M. (2014). Climatological characteristics of atmospheric rivers and their inland penetration over the western United States. *Monthly Weather Review*, *142*(2), 905–921. https://doi.org/10.1175/MWR-D-13-00168.1

Saha, S., Moorthi, S., Pan, H.-L., Wu, X., Wang, J., Nadiga, S., et al. (2010). The NCEP climate forecast system reanalysis. *Bulletin of the American Meteorological Society*, *91*(8), 1015–1058. https://doi.org/10.1175/2010BAMS3001.1

Shields, C. A., Rutz, J. J., Leung, L.-Y., Ralph, F. M., Wehner, M., Kawzenuk, B., et al. (2018). Atmospheric River Tracking Method Intercomparison Project (ARTMIP): Project goals and experimental design. *Geoscientific Model Development*, *11*(6), 2455–2474. https://doi.org/10.5194/gmd-11-2455-2018

Smith, R. B. (1979). The influence of mountains on the atmosphere. *Advances in Geophysics*, *21*, 87–230. https://doi.org/10.1016/S0065-2687(08)60262-9

Wick, G. A., Neiman, P. J., & Ralph, F. M. (2013). Description and validation of an automated objective technique for identification and characterization of the integrated water vapor signature of atmospheric rivers. *IEEE Transactions*, *51*(4), 2166–2176. https://doi.org/10.1109/TGRS.2012.2211024